

## RESEARCH ARTICLE

# Early CD8 T-cell memory precursors and terminal effectors exhibit equipotent *in vivo* degranulation

Yevgeniy Yuzefpolskiy, Florian M. Baumann, Vandana Kalia and Surojit Sarkar

Early after priming, effector CD8 T cells are distinguished into memory precursor and short-lived effector cell subsets (MPECs and SLECs). Here, we delineated a distinct *in vivo* heterogeneity in killer cell lectin-like receptor G1 (KLRG-1) expression, which was strongly associated with diverse MPEC and SLEC fates. These *in vivo* MPECs and SLECs expressed equivalent levels of cytotoxic molecules and effector cytokines. Using a unique *in vivo* degranulation assay, we found that the MPECs and SLECs similarly encountered infected target cells and elaborated equivalent levels of cytotoxicity *in vivo*. These data provide direct *in vivo* evidence that memory-fated cells pass through a robust effector phase. Additionally, the preferential localization of the MPECs in the lymph nodes, where a lesser degree of cytotoxicity was elaborated, suggests that the MPECs may be protected from excessive stimulation and terminal differentiation by virtue of their differential tissue localization. These data provide novel mechanistic insights into the linear decreasing potential model of memory differentiation.

*Cellular & Molecular Immunology* (2015) 12, 400–408; doi:10.1038/cmi.2014.48; published online 28 July 2014

**Keywords:** CD8; MPEC; SLEC; *in vivo*; degranulation; effector; cytotoxicity

## INTRODUCTION

During viral infections, naive CD8 T cells rapidly proliferate and differentiate into effector cells upon receiving optimal T cell receptor, costimulatory and inflammatory signals.<sup>1–4</sup> Once they mediate pathogen clearance, the majority (90%–95%) of the effector cells die *via* apoptosis (referred to as short-lived effector cells, SLECs) and only a small subset survives (referred to as memory precursor effector cells, MPECs) to form a pool of long-lived memory cells. It is now well established that the precursors of memory cells are generated during the effector expansion phase, and the identification of distinctive surface markers that preferentially associate with SLEC or MPEC subsets in early effector cells has seen tremendous advancements during the last decade.<sup>5–9</sup> We and others have shown that *ex vivo* heterogeneity in the killer cell lectin-like receptor G1 (KLRG-1) marks the MPEC and SLEC subsets during the early stages of T-cell expansion (approximately day 4 post-infection and onwards) following a viral infection: KLRG-1<sup>int</sup> cells represent the MPECs and KLRG-1<sup>hi</sup> cells represent the SLEC population.<sup>6,9</sup> This clear distinction of terminal effector and memory fates has enabled further insights

into the mechanisms regulating effector and memory lineage decisions.

There is considerable interest in the field towards understanding the cytotoxic history of the MPEC and SLEC subsets.<sup>10</sup> Two models of memory differentiation are currently prevalent: the linear differentiation model, which posits that memory cells pass through an effector phase and the divergent model, which proposes that terminal effector and memory lineages are distinct and are dictated by distinct instructional cues.<sup>11</sup> Effector CD8 T cells (or cytotoxic T lymphocytes, CTLs) kill infected target cells when they engage with a cognate peptide–MHC-I complex on the surface of the infected cells. Targeted cell killing is mediated by the release of cytotoxic granules (containing effector molecules, such as granzyme B and perforin)<sup>12</sup> from lysosomal compartments of effector CD8 T cells, a process known as degranulation.<sup>13</sup> During the process of degranulation, the lysosomal membrane proteins are transiently translocated to the surface of the CTLs. Hence, the CTLs that have recently degranulated are marked by the cell surface expression of lysosome associated membrane protein-1 (LAMP-1) and LAMP-2 proteins.<sup>14,15</sup> Degranulation has been

Center for Molecular Immunology and Infectious Diseases, Department of Veterinary and Biomedical Sciences and The Huck Institutes of Life Sciences, The Pennsylvania State University, University Park, PA, USA

Correspondence: Dr. S. Sarkar, W209 Millennium Science Complex, The Huck Institutes of Life Sciences, The Pennsylvania State University, University Park, PA 16802, USA.

E-mail: sarkarkalia@gmail.com

Received: 10 Mar 2014; Revised: 12 May 2014; Accepted: 28 May 2014

shown to be a direct measure of killing by CTLs<sup>16</sup> and is considered a more sensitive readout of CTL functioning. Several studies have measured the cytotoxic capabilities of MPECs and SLECs *ex vivo* and have contended that the memory cells pass through a robust effector state.<sup>1,11</sup> In fact, activation of the effector differentiation program has been linked to CD8 T-cell priming and proliferation. However, whether MPECs and SLECs elaborate similar levels of cytotoxicity *in vivo* remains to be investigated. Based on the differential anatomical localization of MPECs and SLECs, it is believed that specialized microniches within tissues may deliver differential signals, such as IL-2, IL-12, antigens, etc.<sup>6,8,9,17–19</sup> and thereby, may imprint different levels of effector differentiation and memory potential in these subsets. In this study, we sought to directly compare the *in vivo* cytotoxic potential of MPECs and SLECs in their physiologically relevant, native infected environment.

To accomplish this goal, we used *in vivo* staining of KLRG-1, LAMP-1 (CD107a) and LAMP-2 (CD107b) proteins to distinguish between MPECs and SLECs *in vivo* while simultaneously measuring their degranulation potential during murine infection with lymphocytic choriomeningitis virus (LCMV). Our studies showed that KLRG-1 heterogeneity is distinguishable *in vivo* in both lymphoid and non-lymphoid tissues and clearly marks the distinct MPEC and SLEC fates. Importantly, *in vivo* degranulation assessments have revealed that MPECs and SLECs possess similar degranulation potencies and mediate the antigen-specific release of cytotoxic granules only in the presence of cognate antigens. Interestingly, lesser degranulation occurred in the lymphoid tissues, where the MPECs preferentially localized, compared to the non-lymphoid tissues. These studies suggest that MPECs and SLECs differentiate into cytotoxic effectors similarly *in vivo* and that the extent of their cytotoxicity is location-dependent. These findings provide direct *in vivo* evidence in support of the linear naïve to effector to memory differentiation model, with increased stimulation leading to decreased memory potential.

## MATERIALS AND METHODS

### Mice

C57BL/6 mice (Thy1.2<sup>+</sup>) were purchased from the Jackson Laboratory (Bar Harbor, ME, USA). Thy1.1<sup>+</sup> P14 mice bearing the D<sup>b</sup>GP33-specific T cell receptor were fully backcrossed to the C57BL/6 mice and were maintained in our animal colony. All of the animals were used in accordance with the University Institutional Animal Care and Use Committee guidelines.

### Virus and infections

The Armstrong strain of LCMV was propagated, titered and used as previously described.<sup>8</sup> The mice were directly infected with 2×10<sup>5</sup> pfu of LCMV intraperitoneally, and the viral loads were determined at the indicated times as described previously.<sup>8</sup>

### Antibodies, *in vivo* KLRG-1 staining and flow cytometry

All of the antibodies were purchased from Biolegend (San Diego, CA, USA) with the exception of CD107b PE (clone ABL-93), which was procured from Santa Cruz Biotechnology.

Anti-CD107a PE (clone 1D4B) and CD107b PE antibodies were used together in the presence of monensin to measure the *in vivo* degranulation. For the *in vivo* staining of KLRG-1 and CD27, 50 µg of each antibody was administered intravenously, and the lymphocytes were isolated from the indicated tissues 2 h later. The cells were then stained with CD8 and Thy1.1 antibodies and fixed with paraformaldehyde prior to the analysis by flow cytometry. For the analysis of the intracellular cytokines, 10<sup>6</sup> lymphocytes were stimulated with 0.2 µg/ml of GP33-41 peptide in the presence of brefeldin A for 5 h, followed by surface staining for CD8 and Ly5.1 and intracellular staining for interferon (IFN)-γ, tumor-necrosis factor (TNF)-α or IL-2. The *ex vivo* staining of the cells for surface or intracellular proteins and cytokines was conducted as previously described.<sup>8</sup>

For the isolation of day 4.5 MPECs and SLECs, P14 chimeric mice containing 1×10<sup>5</sup> naïve antigen-specific CD8 T cells were infected with LCMV. The donor cells were distinguished in the recipient C57Bl/6 mice by expression of the congenic marker Thy1.1. The MPECs and SLECs were FACS purified using KLRG-1 as a distinguishing marker as described previously.<sup>9</sup> Following FACS purification, approximately 1×10<sup>6</sup> purified KLRG-1<sup>hi</sup> and KLRG-1<sup>int</sup> CD8 T cells were adoptively transferred into infection-matched mice and longitudinally followed in the blood.

### *In vivo* degranulation assay

To measure the *in vivo* degranulation of MPECs and SLECs, C57Bl/6 mice that were infected with LCMV 4.5 or 8 days previously were injected with 50 µg each of CD107a/b PE (or the isotype control) and KLRG-1 APC antibodies along with 10 µg of monensin per mouse. One or two hours later, the mice were killed and stained *ex vivo* with CD8 and Thy1.1 gating antibodies. The paraformaldehyde fixed samples were analyzed with flow cytometry.

### Statistical analysis

Paired or unpaired Student's *t*-tests (two-tailed) were used as indicated to evaluate the differences between the sample mean values. All of the statistical analyses were performed using Prism 5, and the *P* values of statistical significance are depicted by an asterisk according to the Michelin guide scale: \**P*≤0.05, \*\**P*≤0.01 and \*\*\**P*≤0.001, and *P*>0.05 was considered not significant (ns).

## RESULTS

### Distinct *in vivo* heterogeneity in KLRG-1 expression on early effector CD8 T cells

Effector CD8 T cells exhibit heterogeneity in the expression of cell surface markers, such as KLRG-1, IL-2Rα and IL-7Rα, during the activation and expansion phases.<sup>5–9</sup> Differential expression of these proteins has been shown to distinguish between MPEC and SLEC subsets with divergent memory and terminal effector fates, respectively. To determine if heterogeneity in the expanding effector CD8 T-cell population is also distinguishable *in vivo*, we performed an *in vivo* staining of

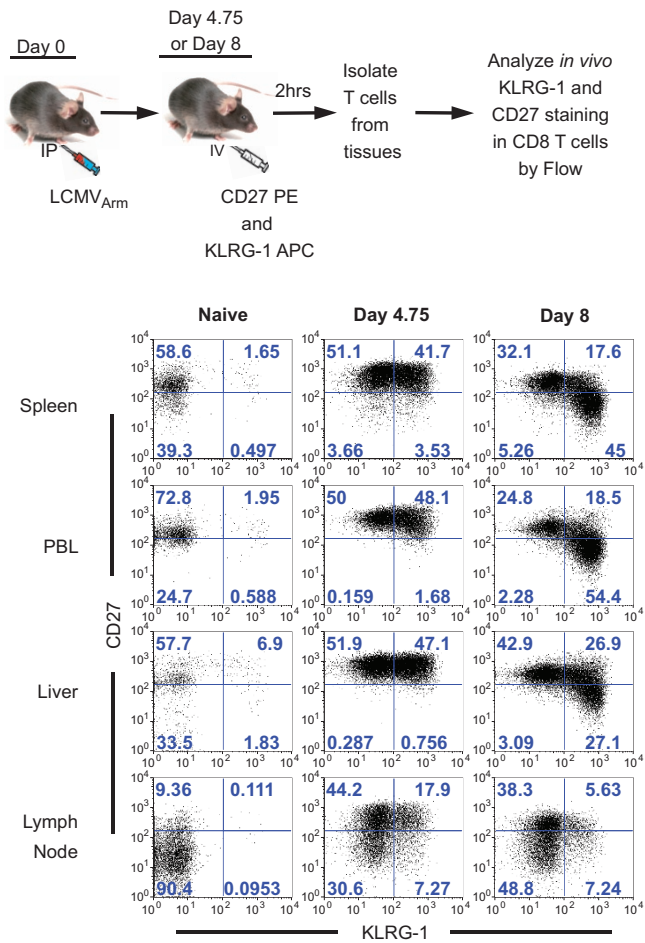


**Figure 1** Early effector CD8 T cells show distinct *in vivo* heterogeneity in KLRG-1 expression in lymphoid and non-lymphoid tissues. P14 chimeric mice containing  $10^5$  D<sup>b</sup>GP33-specific CD8 T cells were infected with LCMV. At 4.75 or 8 days after infection, mice were injected intravenously with 50  $\mu$ g of CD27 PE or KLRG-1 APC antibodies. After 2 h, lymphocytes were isolated from the indicated tissues, stained *ex vivo* for CD8 and Thy1.1 and analyzed by flow cytometry. CD8 and Thy1.1 were used as gating markers. KLRG-1, killer cell lectin-like receptor G1; LCMV, lymphocytic choriomeningitis virus.

the cell surface markers KLRG-1 (typically associated with terminally differentiated CD8 T cells) and CD27 (typically expressed at higher levels on activated and memory cells) by the intravenous administration of fluorescently labeled antibodies (Figure 1) in LCMV-infected mice at 4.75 and 8 days after infection. Such *in vivo* delineation of heterogeneity in the expression of the markers associated with diverse cell fates would allow for the direct analysis of effector CD8 T-cell subsets in their native environment.

Consistent with previous *ex vivo* staining data,<sup>6,9</sup> we found that antigen-specific effector CD8 T cells also showed an evident *in vivo* heterogeneity in the expression of KLRG-1 during early (day 4.75) and peak (day 8) expansion in both secondary lymphoid (spleen and lymph nodes) and non-lymphoid (liver) tissues. CD27 expression increased after activation and was uniformly high on the day 4.75 effectors (Figure 1). However, the KLRG-1<sup>hi</sup> effectors expressed lower levels of CD27 at 8 days after

infection. Notably, the balance of KLRG-1<sup>int</sup> and KLRG-1<sup>hi</sup> effectors was distinctive in the lymph nodes, with the majority of the lymph node-derived effector cells binding lower levels of anti-KLRG-1 antibodies at both 4.5 and 8 days after infection (Figure 1). In each tissue analyzed, the proportions of the KLRG-1<sup>int</sup> and KLRG-1<sup>hi</sup> effector subsets were similar using both *in vivo* and *ex vivo* staining methods. Additionally, the mean fluorescence intensity (MFI) of the KLRG-1 antibody staining was also largely similar for both subsets in all of the tissues analyzed (Supplementary Figure 1). These data suggest that the decreased proportions of KLRG-1<sup>hi</sup> antigen-specific CD8 T cells observed in the lymph nodes using *in vivo* staining were apparently independent of the confounding issues related to reduced antibody access in the lymph nodes. Notably, the KLRG-1<sup>int</sup> antigen-specific CD8 T cells were enriched in the lymph nodes at all of the time points analyzed after infection (Supplementary Figure 2). Together, these data demonstrate an evident *in vivo* KLRG-1 heterogeneity in effector CD8 T cells during the early and late stages of expansion, with the lymph nodes being distinctly populated with putatively less differentiated KLRG-1<sup>int</sup> effector cells.

### *In vivo* heterogeneity of KLRG-1 distinguishes memory and terminal effector fates

A higher KLRG-1 expression level in the direct *ex vivo* stains has typically been associated with more terminally differentiated cells, such that the differential expression of KLRG-1 marks the diverse memory and death fates of the effector CD8 T cells.<sup>6,9</sup> We next assessed the fates associated with the *in vivo* stained KLRG-1<sup>int</sup> and KLRG-1<sup>hi</sup> effector cells. The *in vivo* stained effector CD8 T cells were FACS purified at day 4.5 after infection and were adoptively transferred into infection-matched recipient mice. Infection-matched congenitally distinct mice were employed as recipients to ensure that the donor cells differentiated in similarly infected environments from where they were purified. The donor cells were followed longitudinally in the blood, and the final numbers were determined at memory. As shown in Figure 2a, both effector subsets continued to expand to similar extents after transfer and increased their numbers by approximately 10-fold until the peak of the effector responses. However, following antigen clearance, the KLRG-1<sup>int</sup> subset underwent a lesser degree of contraction and preferentially survived into the memory phase compared to the KLRG-1<sup>hi</sup> effectors. Following contraction, the final numbers of KLRG-1<sup>int</sup> donor cells were also significantly higher in all lymphoid and non-lymphoid tissues analyzed at memory (Figure 2b). At the peak of the donor cell expansion, neither subset of the unstained donor cells had any of the remaining original KLRG-1 antibody stain that was used for sorting (data not shown). Thus, the KLRG-1<sup>int</sup> and KLRG-1<sup>hi</sup> donors underwent contraction and began to exhibit survival differences >5 days after the adoptive transfer when no detectable cell surface bound antibodies remained, suggesting that the differences in cell survivability were likely independent of the differential levels of cell

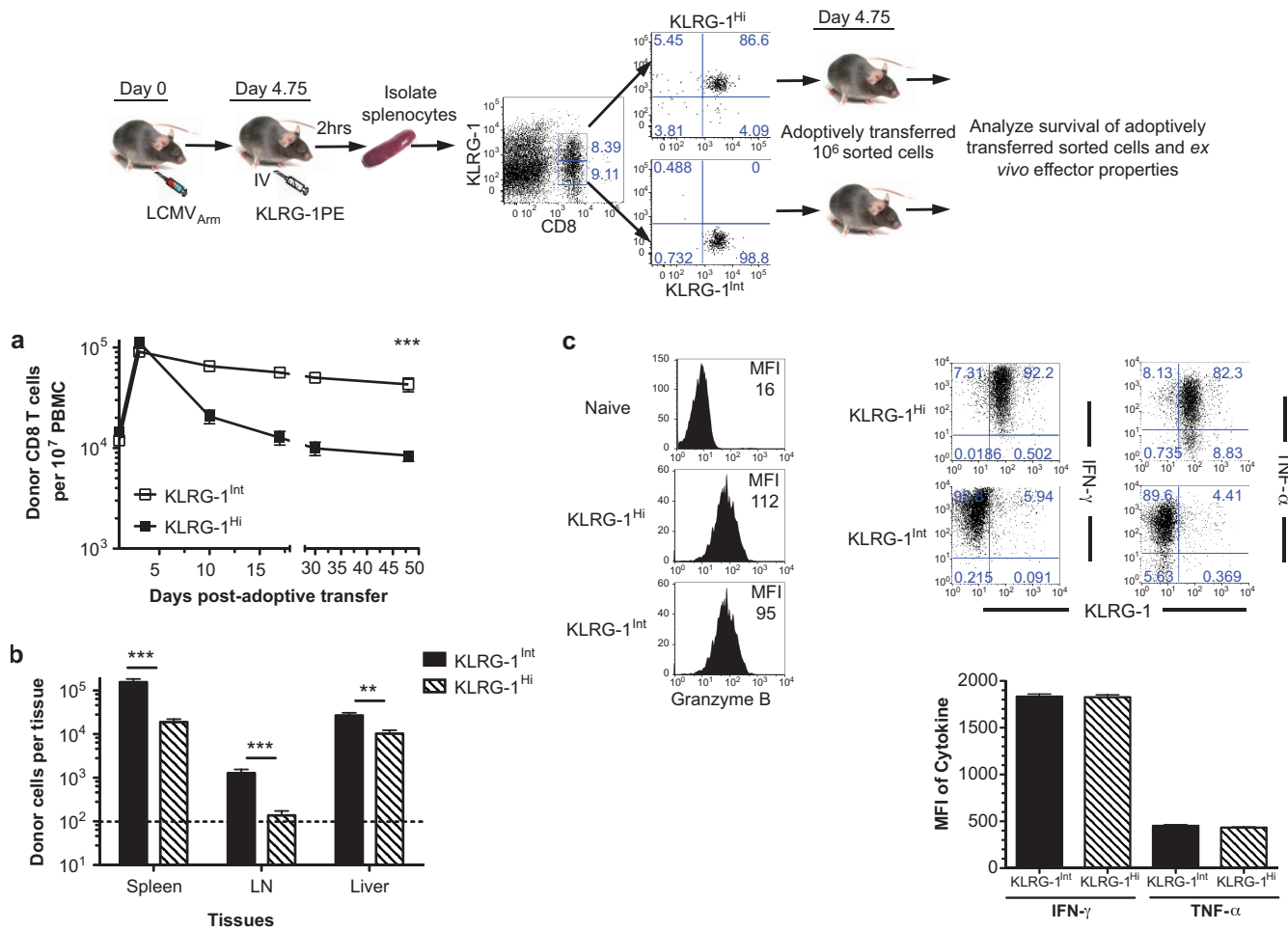


**Figure 2** *In vivo* stained KLRG-1 heterogeneous effectors represent the MPEC and SLEC populations that express similar levels of effector molecules. At day 4.75 after the LCMV infection, splenocytes were isolated from the P14 chimeric mice that had been stained for KLRG-1 PE *in vivo* as described in Figure 1. The CD8<sup>+</sup> T cells were sorted into KLRG-1<sup>int</sup> and KLRG-1<sup>hi</sup> subsets, and approximately 1 × 10<sup>6</sup> donor cells were adoptively transferred into congenically mismatched C57Bl/6 recipient mice that had been infected with LCMV 4.75 days earlier (infection-matched recipients). (a) Antigen-specific donor CD8 T cells were analyzed in the PBMCs of the recipient mice at the indicated days after the adoptive transfer and are presented as line graphs. The average ± s.e.m. values are plotted from two independent repeats. Unpaired Student's *t*-tests were used for the analysis of statistical significance, and *P* < 0.001 is depicted by \*\*\*. (b) The KLRG-1<sup>int</sup> and KLRG-1<sup>hi</sup> donor cells were enumerated in the indicated tissues at approximately day 50 after the adoptive transfer by a flow cytometry analysis of the CD8<sup>+</sup>Thy1.1<sup>+</sup> T cells. The bar graphs show the average number of donor cells at memory ± s.e.m. Unpaired Student's *t*-tests were used for the analysis of statistically significant differences between the KLRG-1<sup>int</sup> and KLRG-1<sup>hi</sup> groups (\**P* ≤ 0.05, \*\**P* ≤ 0.01, \*\*\**P* ≤ 0.001). The *in vivo* stained effector CD8 T cells from the day 4.75 LCMV-infected P14 chimeric mice were FACS purified into KLRG-1<sup>int</sup> and KLRG-1<sup>hi</sup> subsets. (c) The level of granzyme B expression in both subsets was assessed by *ex vivo* intracellular staining and a flow cytometry analysis. Histogram plots with the MFI of granzyme B expression are shown. (d) The purified effector subsets were also stimulated with 0.2 μg/ml of GP33-41 peptide for 5 h in the presence of brefeldin A, followed by intracellular cytokine staining for IFN- $\gamma$  and TNF- $\alpha$ . The MFIs of the indicated cytokines that were stained in both effector subsets are presented as bar graphs. FACS, fluorescence-activated cell sorting; KLRG-1, killer cell lectin-like receptor G1; LCMV, lymphocytic choriomeningitis virus; MFI, mean fluorescence intensity; MPEC, memory precursor effector cell; PBMC, peripheral blood mononuclear cell; SLEC, short-lived effector cell.

surface bound KLRG-1 antibodies used during FACS purification. Consistent with *ex vivo* studies,<sup>6,9</sup> these data clearly demonstrate that *in vivo* effector cell heterogeneity in KLRG-1 expression marks distinct MPEC and SLEC fates.

### Similar expression of effector molecules in the *in vivo* stained MPECs and SLECs

Having thus devised and validated a method of delineating MPECs and SLECs *in vivo*, we next sought to understand the differentiation paths of MPECs and SLECs *in vivo* in their

native environment. Memory cells have been proposed to differentiate from less differentiated effector cells<sup>20,21</sup> or in cases to even bypass the effector differentiation stage.<sup>22,23</sup> To compare the effector status of the *in vivo* stained MPECs and SLECs, we first measured the expression levels of the key effector molecule granzyme B and the effector cytokines IFN- $\gamma$  and TNF- $\alpha$ . Both *in vivo* marked subsets expressed similar levels of the intracellular granzyme B (Figure 2c) directly *ex vivo*. Notably, MPECs and SLECs that were purified and stained *in vivo* also expressed similar levels of the effector cytokines IFN- $\gamma$  and TNF- $\alpha$ , after

5 h of *in vitro* peptide stimulation, on a per cell basis (Figure 2d). These data indicate that both MPECs and SLECs express effector molecules similarly.

### MPECs and SLECs degranulate to a similar extent *in vivo* in an antigen-dependent manner

To directly assess the *in vivo* cytotoxic functions of MPECs and SLECs, we employed a unique *in vivo* degranulation assay to measure the extent of cytotoxic granule release by the effector

subsets in their native physiological environment. The assay involved direct *in vivo* administration of the KLRG-1 antibody to distinguish between the MPECs and SLECs, along with CD107a/b antibodies to determine the extent of degranulation (Figure 3). Optimal *in vivo* antibody staining with a good correlation with *ex vivo* staining required an incubation time of approximately 1 h for the antibodies to reach dynamic equilibrium following egress from the vasculature and accessibility of the target cells. Thus, *in vivo* degranulation was assessed

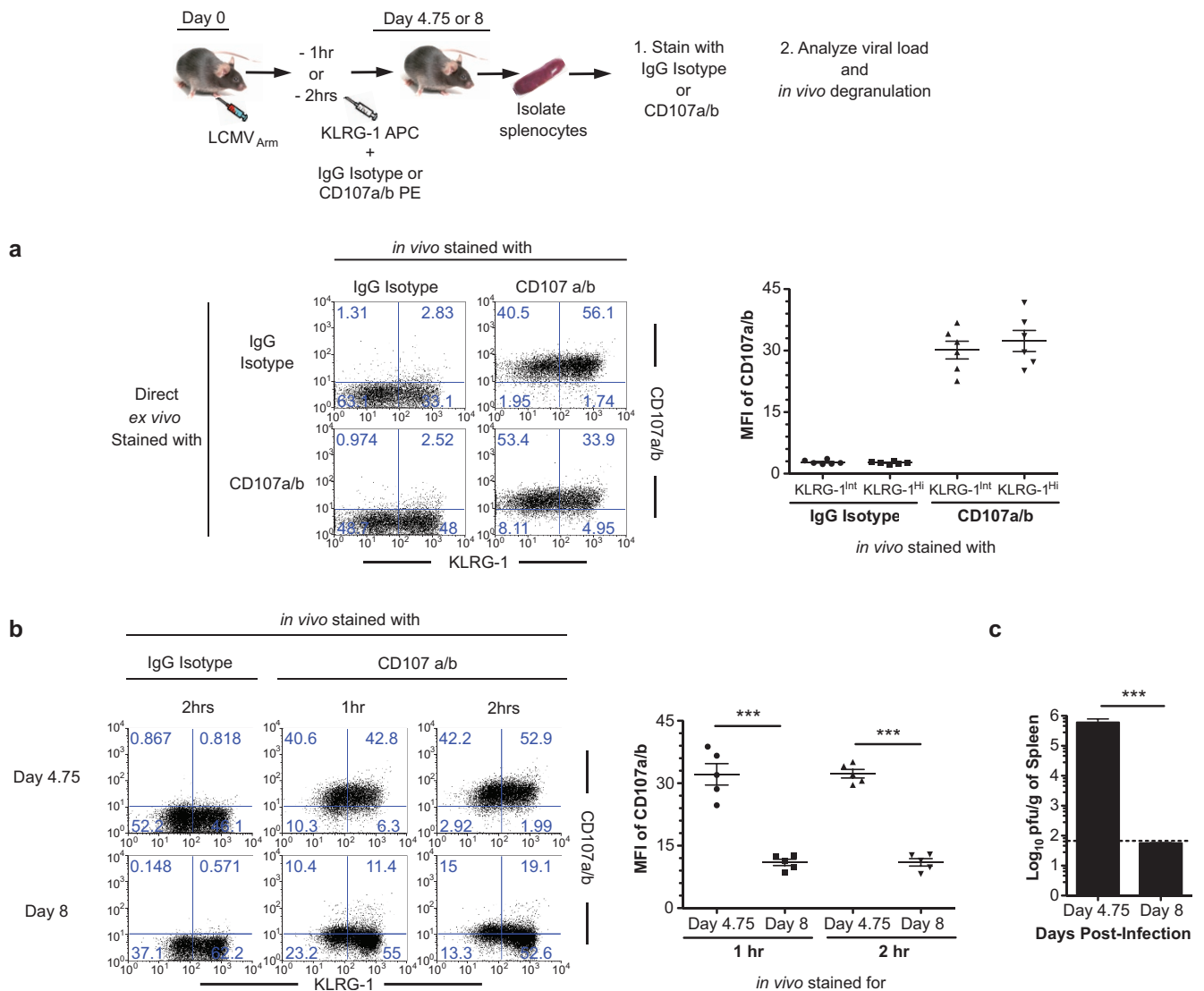


**Figure 3** The MPECs and SLECs degranulate to a similar extent *in vivo*, as determined by the presence of antigens. The KLRG-1<sup>int</sup> MPECs and the KLRG-1<sup>hi</sup> SLECs were assessed for their rate of degranulation *in vivo* by intravenous injection of 50  $\mu$ g of KLRG-1 APC and CD107a/b PE antibodies in P14 chimeric mice that had been infected with LCMV 4.75 days previously. One control set of mice were injected with IgG PE as the isotype control instead of the CD107a/b antibodies. Two hours after the antibody injection, the mice were killed, and the splenocytes were isolated and stained *ex vivo* with CD8, Thy1.1, the IgG isotype control or CD107a/b antibodies. **(a)** Representative FACS plots and summary dot plots showing the mean  $\pm$  s.e.m. MFI of the CD107a/b staining from two independent experiments are presented. **(b)** The *in vivo* degranulation of the MPECs and SLECs was compared at days 4.75 and 8 after LCMV infection in P14 chimeric mice. Representative FACS plots and dot plots summarizing the CD107a/b MFI are presented. Whether the difference in the mean values between the indicated groups was significant was determined using Student's unpaired *t*-test (\* $P \leq 0.05$ , \*\* $P \leq 0.01$ , \*\*\* $P \leq 0.001$ ). **(c)** The viral loads in the spleens of the mice infected with LCMV at days 4.75 and 8 are presented as bar graphs. The mean  $\pm$  s.e.m. are presented, and \*\*\* represents  $P \leq 0.001$ . FACS, fluorescence-activated cell sorting; KLRG-1, killer cell lectin-like receptor G1; LCMV, lymphocytic choriomeningitis virus; MFI, mean fluorescence intensity; MPEC, memory precursor effector cell; PBMC, peripheral blood mononuclear cell; SLEC, short-lived effector cell.

using 1 h and 2 h incubation times. The CD107a/b staining was only seen when the antibodies were administered *in vivo*. Splenocytes isolated without the *in vivo* staining (isotype control) of CD107a/b did not exhibit positive staining when stained for CD107a/b directly *ex vivo* (Figure 3a). This lack of CD107a/b staining on the day 4.75 effectors *ex vivo* in the absence of restimulation indicated that this assay measures the degranulation of cells following *in vivo* antigen stimulation. Importantly, the level of CD107a/b staining following the *in vivo* administration of the antibodies, as assessed by MFI of the

CD107a/b staining, was similar in both the MPECs and SLECs (Figure 3a). These data demonstrate that there is an equivalent antigenic encounter and elaboration of cytotoxic function by MPECs and SLECs *in vivo*.

To further investigate the role of antigen and to assess the antigenic encounter history of MPECs and SLECs in our *in vivo* degranulation experiments, we compared *in vivo* CD107a/b staining on days 4.75 (when the systemic antigen was present) and 8 after infection (when LCMV was largely cleared from the system). The extent of the *in vivo* degranulation was similar in

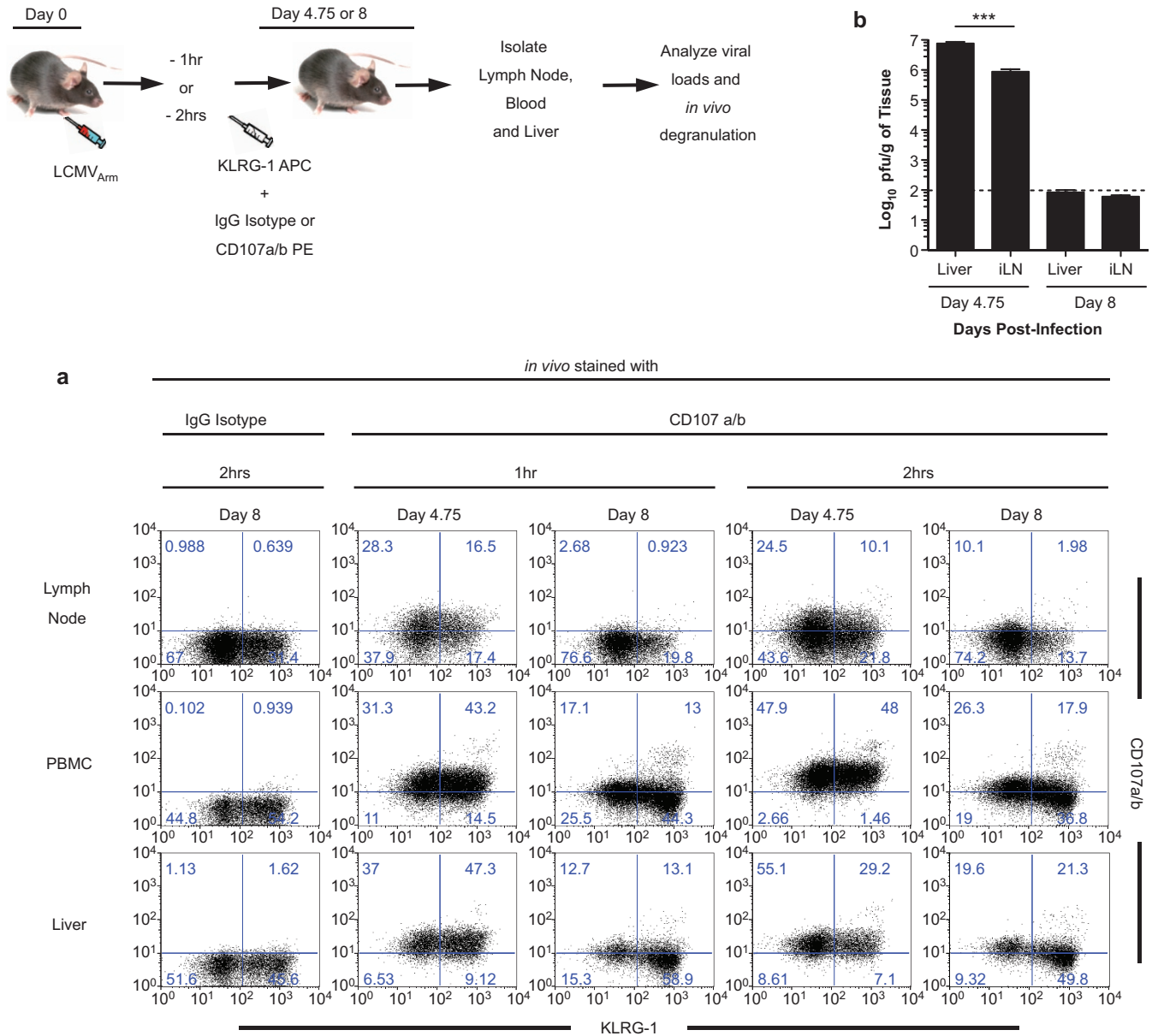


**Figure 4** Effector CD8 T cells degranulate to a higher extent in non-lymphoid tissues than in lymphoid tissues. The *in vivo* degranulation of effector cells was compared at days 4.75 and 8 after LCMV infection in the lymph nodes, PBMCs and the liver. The mice were killed, their tissues were isolated and antigen-specific CD8 T cells were stained *ex vivo* for the gating markers CD8 and Thy1.1 at 1 h or 2 h after the *in vivo* injection of the CD107a/b and KLRG-1 antibodies. The level of degranulation was assessed using flow cytometry. Representative FACS plots from two independent experiments are presented. FACS, fluorescence-activated cell sorting; KLRG-1, killer cell lectin-like receptor G1; LCMV, lymphocytic choriome-ningitis virus; MPEC, memory precursor effector cell; PBMC, peripheral blood mononuclear cell; SLEC, short-lived effector cell.

the 1 and 2 hour assay times (Figure 3b), indicating the rapid release of cytotoxic granules following an antigenic encounter by CTLs so that the maximal level of degranulation was achieved within 1 h. Notably, the day 4.75 effectors indeed degranulated more than the day 8 effectors, as determined by the MFI of the *in vivo* stained CD107a/b (Figure 3b). These differences in antigen encounters and CTL function at days 4.75 and 8 post-infection clearly correlated with the differential viral loads in the spleen (Figure 3c). Thus, the *in vivo* staining of CD107a/b in the MPECs and SLECs measures antigen-dependent cytotoxic granule release in the native environment and reveals evident similarities in their *in vivo* cytotoxic potential.

### CTLs degranulate more in non-lymphoid tissues than in lymphoid tissues

The data presented in Figures 2 and 3 demonstrate that FACS purified *in vivo* stained KLRG-1<sup>int</sup> and KLRG-1<sup>hi</sup> antigen-specific CD8 T cells from the spleen possess diverse fates despite elaborating similar degranulation in response to antigenic stimulation in the spleen. Based on (i) the increased prevalence of KLRG-1<sup>int</sup> cells in the lymph nodes (Figure 1 and Supplementary Figures 1 and 2) at all time-points post-infection; (ii) the preferential localization of the KLRG-1<sup>int</sup> donors in the lymph nodes rather than the KLRG-1<sup>hi</sup> donor cells shortly after the adoptive transfer into infection-matched recipients;<sup>9</sup> and (iii) previous reports that lymph node-derived effector CD8 T cells enter the memory pool more readily than spleen derived effectors,<sup>24</sup> we next compared the *in vivo* degranulation of the MPECs and SLECs in lymph nodes and in peripheral sites, such as the liver. As observed in splenocytes (Figure 3), the day 4.75 effectors degranulated more than the day 8 effectors in all other tissue sites analyzed as well (Figure 4). Moreover, the degranulation readouts were largely similar at the 1 and 2 h assay times, as observed previously (Figure 3), indicating rapid degranulation after stimulation. Surprisingly, we found an evident difference in the level of effector cell degranulation in the lymphoid tissues compared to the non-lymphoid tissues (Figure 4). Both the day 4.75 and 8 effectors exhibited more degranulation in the liver than in the lymph nodes. In general, the viral loads in the inguinal lymph nodes were approximately 10-fold lower than in the liver after intraperitoneal acute infection with LCMV at approximately day 4.5 after infection, and all of the tissues were largely cleared of plaqueable virus at day 8 after infection (Figure 4b). These data are consistent with the measurable differences in the *in vivo* antigenic encounters and degranulation between day 4.5 and day 8 after infection as well as the lesser degree of degranulation observed in the inguinal lymph node.

Overall, both MPECs and SLECs exhibited decreased degranulation at day 8 in all of the tissues analyzed. This correlated with LCMV loads several logs lower at day 8 compared to day 4.75 post-infection (Figure 4c). However, compared to day 4.75, when MPECs and SLECs exhibited similarly potent *in vivo* degranulation in all of the tissues analyzed (Figures 3 and 4), MPECs shut down their effector functions more effectively in the inguinal lymph nodes at day 8 post-infection. This

may be related to a more rapid viral clearance from the inguinal lymph nodes compared to the liver or spleen. Indeed, as shown in Figure 4b, lower LCMV loads were observed in the inguinal lymph nodes compared to the liver at day 4.75 after infection. Nevertheless, measurable degranulation was still observed at day 8 in the liver and in PBMCs (Figure 4c), and MPECs had modestly more degranulation than SLECs. While these differences are subtle, they are indicative of the continued differentiation of the KLRG-1<sup>int</sup> effector cells into more terminally differentiated KLRG-1<sup>hi</sup> cells in peripheral sites due to residual antigenic stimulation. Slightly lower levels of degranulation of SLECs may be related to a possible functional exhaustion of SLECs due to prolonged antigenic stimulation in the peripheral sites. Collectively, these data demonstrate an increased antigenic stimulation in the peripheral sites, thereby resulting in greater terminal effector differentiation.

### DISCUSSION

Collectively, these data provide strong *in vivo* evidence of MPEC and SLEC heterogeneity and direct *in vivo* proof that memory cells pass through a potent effector phase in the presence of antigens. Whether differentiation through an effector phase is obligatory for the development of memory cells remains to be determined. Indeed, it has been proposed that differentiation through an effector phase may result in epigenetic changes at critical effector gene loci that allow memory cells to remain in a 'poised' state to react swiftly following a secondary antigenic encounter.

Effector differentiation is closely tied to CD8 T-cell proliferation after priming. Using a unique *in vivo* degranulation assay, we showed that MPECs and SLECs encounter antigens similarly in the spleen and are capable of exerting cytotoxicity similarly *in vivo*. Using an *in vitro* degranulation assay, Wolint *et al.*<sup>13</sup> have previously reported a progressive increase in effector CTL degranulation with increasing duration of stimulation with a cognate peptide antigen so that the frequency of the degranulating cells doubled when the stimulation times were increased from 1 h to 2 h and reached maximal levels at approximately 5–6 h. In contrast, we observed rapid *in vivo* degranulation with maximal levels within 1 h after stimulation and with no significant increase in the extent of degranulation when the assay time was increased to 2 h. This may be related to a more efficient antigen presentation *in vivo*, potentially due to distinct inflammatory stimulation milieu. Moreover, these data indicate that a 1 h incubation time is sufficient for the antibodies to egress from the vasculature and to stain the cells in their microenvironmental niche in the non-lymphoid and secondary lymphoid tissues. Based on a recent report by Anderson *et al.*<sup>25,26</sup> stating that perfusion is inefficient at removing blood-borne lymphocytes from non-lymphoid peripheral organs, such as the lungs, it is possible that in the case of the liver, our *in vivo* staining readouts are reflective of both intravascular and tissue-resident lymphocytes.

Together with tissue localization data, these studies indicate that despite possessing similar cytotoxic potentials, MPECs exert less cytotoxicity *in vivo* by virtue of preferential localization to

the secondary lymphoid tissues with relatively lower antigen levels. It is conceivable that memory-fated cells manage to escape rapid and recurring degranulation *in vivo* during an infection and hence emerge as a metabolically fit population that has conserved its resources to survive long-term. These conclusions are supported by previous studies proposing that MPECs shut down their effector functions more rapidly<sup>17</sup> and that lymph node-derived effector cells preferentially enter the memory pool compared to spleen-derived effector cells.<sup>24</sup> Several studies have shown that CD8 T cells that are activated relatively later during an immune response are less stimulated and preferentially differentiate into memory cells.<sup>1,27–29</sup> In contrast, we have shown that a prolonged antigenic stimulation leads to the generation of KLRG-1<sup>hi</sup> SLECs.<sup>9</sup> Our current findings of the preferential localization of SLECs in non-lymphoid sites suggest that SLECs putatively mount increased rounds of killing after continually encountering antigens in peripheral sites, thereby undergoing terminal differentiation. These findings lend support to the decreasing potential model of memory differentiation, which posits that the potential of effector cells to differentiate into memory cells decreases progressively with increasing antigenic stimulation. Our data suggest that the increased antigenic stimulation of effector cells in peripheral sites may be a means of driving terminal effector differentiation: KLRG-1<sup>int</sup> effectors may be driven towards a KLRG-1<sup>hi</sup> terminally differentiated state due to repetitive antigenic encounters in peripheral sites, such as the liver and lungs, and KLRG-1<sup>hi</sup> cells may be driven towards functional exhaustion. These findings lay the groundwork for more detailed functional, phenotypic and microarray investigations into the putative functional exhaustion of KLRG-1<sup>hi</sup> cells, possibly due to increased antigenic encounters and related proliferation during the late stages of infection. The rapid shutdown of effector functions by MPECs in the lymph nodes, but the prolonged degranulation of the KLRG-1<sup>int</sup> cells at day 8 in the liver further suggests that the KLRG-1<sup>int</sup> effector subsets in the liver may be compromised in their ability to contribute to the long-lived pool of memory cells compared to the KLRG-1<sup>int</sup> effector cells in the inguinal lymph nodes. Thus, by using a unique assay to measure the *in vivo* cytotoxicity of MPECs and SLECs, the current study provides insight into the mechanisms of CD8 T-cell memory differentiation. A clear understanding of the *in vivo* events regulating effector and memory lineages has a direct bearing on vaccine-induced immunological memory.

## ACKNOWLEDGEMENTS

This work was supported in part by research funding from the Pennsylvania State University to SS and VK.

Supplementary Information accompanies the paper on *Cellular & Molecular Immunology's* website. (<http://www.nature.com/cmi>).

1 Kalia V, Sarkar S, Ahmed R. CD8 T-cell memory differentiation during acute and chronic viral infections. *Adv Exp Med Biol* 2010; **684**: 79–95. E

- 2 Arens R, Schoenberger SP. Plasticity in programming of effector and memory CD8 T-cell formation. *Immunity Rev* 2010; **235**: 190–205.
- 3 Belz GT, Kallies A. Effector and memory CD8<sup>+</sup> T cell differentiation: toward a molecular understanding of fate determination. *Curr Opin Immunol* 2010; **22**: 279–285.
- 4 Zhang N, Bevan MJ. CD8<sup>+</sup> T cells: foot soldiers of the immune system. *Immunity* 2011; **35**: 161–168.
- 5 Huster KM, Busch V, Schiemann M, Linkemann K, Kerksiek KM, Wagner H *et al*. Selective expression of IL-7 receptor on memory T cells identifies early CD40L-dependent generation of distinct CD8<sup>+</sup> memory T cell subsets. *Proc Natl Acad Sci USA* 2004; **101**: 5610–5615.
- 6 Joshi NS, Cui W, Chandele A, Lee HK, Urso DR, Hageman J *et al*. Inflammation directs memory precursor and short-lived effector CD8<sup>+</sup> T cell fates *via* the graded expression of T-bet transcription factor. *Immunity* 2007; **27**: 281–295.
- 7 Kaech SM, Tan JT, Wherry EJ, Konieczny BT, Surh CD, Ahmed R. Selective expression of the interleukin 7 receptor identifies effector CD8 T cells that give rise to long-lived memory cells. *Nat Immunol* 2003; **4**: 1191–1198.
- 8 Kalia V, Sarkar S, Subramaniam S, Haining WN, Smith KA, Ahmed R. Prolonged interleukin-2R $\alpha$  expression on virus-specific CD8<sup>+</sup> T cells favors terminal-effector differentiation *in vivo*. *Immunity* 2010; **32**: 91–103.
- 9 Sarkar S, Kalia V, Haining WN, Konieczny BT, Subramaniam S, Ahmed R. Functional and genomic profiling of effector CD8 T cell subsets with distinct memory fates. *J Exp Med* 2008; **205**: 625–640.
- 10 Lefrancois L, Obar JJ. Once a killer, always a killer: from cytotoxic T cell to memory cell. *Immunity Rev* 2010; **235**: 206–218.
- 11 Kalia V, Sarkar S, Gourley TS, Rouse BT, Ahmed R. Differentiation of memory B and T cells. *Curr Opin Immunol* 2006; **18**: 255–264.
- 12 Kagi D, Ledermann B, Burki K, Seiler P, Odermatt B, Olsen KJ *et al*. Cytotoxicity mediated by T cells and natural killer cells is greatly impaired in perforin-deficient mice. *Nature* 1994; **369**: 31–37.
- 13 Wolint P, Betts MR, Koup RA, Oxenius A. Immediate cytotoxicity but not degranulation distinguishes effector and memory subsets of CD8<sup>+</sup> T cells. *J Exp Med* 2004; **199**: 925–936.
- 14 Krzewski K, Gil-Krzewska A, Nguyen V, Peruzzi G, Coligan JE. LAMP1/CD107a is required for efficient perforin delivery to lytic granules and NK-cell cytotoxicity. *Blood* 2013; **121**: 4672–4683.
- 15 Liu D, Bryceon YT, Meckel T, Vasiliver-Shamis G, Dustin ML, Long EO. Integrin-dependent organization and bidirectional vesicular traffic at cytotoxic immune synapses. *Immunity* 2009; **31**: 99–109.
- 16 Aktas E, Kucuksezer UC, Bilgic S, Erten G, Deniz G. Relationship between CD107a expression and cytotoxic activity. *Cell Immunol* 2009; **254**: 149–154.
- 17 Obar JJ, Jellison ER, Sheridan BS, Blair DA, Pham QM, Zickovich JM *et al*. Pathogen-induced inflammatory environment controls effector and memory CD8<sup>+</sup> T cell differentiation. *J Immunol* 2011; **187**: 4967–4978.
- 18 Obar JJ, Molloy MJ, Jellison ER, Stoklasek TA, Zhang W, Usherwood EJ *et al*. CD4<sup>+</sup> T cell regulation of CD25 expression controls development of short-lived effector CD8<sup>+</sup> T cells in primary and secondary responses. *Proc Natl Acad Sci USA* 2010; **107**: 193–198.
- 19 Pipkin ME, Sacks JA, Cruz-Guilloty F, Lichtenheld MG, Bevan MJ, Rao A. Interleukin-2 and inflammation induce distinct transcriptional programs that promote the differentiation of effector cytolytic T cells. *Immunity* 2010; **32**: 79–90.
- 20 Bannard O, Kraman M, Fearon DT. Secondary replicative function of CD8<sup>+</sup> T cells that had developed an effector phenotype. *Science* 2009; **323**: 505–509.
- 21 Jacob J, Baltimore D. Modelling T-cell memory by genetic marking of memory T cells *in vivo*. *Nature* 1999; **399**: 593–597.
- 22 Manjunath N, Shankar P, Wan J, Weninger W, Crowley MA, Hieshima K *et al*. Effector differentiation is not prerequisite for generation of memory cytotoxic T lymphocytes. *J Clin Invest* 2001; **108**: 871–878.
- 23 Lauvau G, Vijn S, Kong P, Horng T, Kerksiek K, Serbina N *et al*. Priming of memory but not effector CD8 T cells by a killed bacterial vaccine. *Science* 2001; **294**: 1735–1739.
- 24 Kedzierska K, Stambas J, Jenkins MR, Keating R, Turner SJ, Doherty PC. Location rather than CD62L phenotype is critical in the early



- establishment of influenza-specific CD8<sup>+</sup> T cell memory. *Proc Natl Acad Sci USA* 2007; **104**: 9782–9787.
- 25 Anderson KG, Mayer-Barber K, Sung H, Beura L, James BR, Taylor JJ *et al*. Intravascular staining for discrimination of vascular and tissue leukocytes. *Nat Protoc* 2014; **9**: 209–222.
- 26 Anderson KG, Sung H, Skon CN, Lefrancois L, Deisinger A, Vezys V *et al*. Cutting edge: intravascular staining redefines lung CD8 T cell responses. *J Immunol* 2012; **189**: 2702–2706.
- 27 D'Souza WN, Hedrick SM. Cutting edge: latecomer CD8 T cells are imprinted with a unique differentiation program. *J Immunol* 2006; **177**: 777–781.
- 28 Sarkar S, Teichgraber V, Kalia V, Polley A, Masopust D, Harrington LE *et al*. Strength of stimulus and clonal competition impact the rate of memory CD8 T cell differentiation. *J Immunol* 2007; **179**: 6704–6714.
- 29 van Faassen H, Saldanha M, Gilbertson D, Dudani R, Krishnan L, Sad S. Reducing the stimulation of CD8<sup>+</sup> T cells during infection with intracellular bacteria promotes differentiation primarily into a central (CD62L<sup>high</sup>CD44<sup>high</sup>) subset. *J Immunol* 2005; **174**: 5341–5350.



This work is licensed under a Creative Commons Attribution-NonCommercial-ShareAlike 3.0 Unported License. The images or other third party material in this article are included in the article's Creative Commons license, unless indicated otherwise in the credit line; if the material is not included under the Creative Commons license, users will need to obtain permission from the license holder to reproduce the material. To view a copy of this license, visit <http://creativecommons.org/licenses/by-nc-sa/3.0/>